論文 / 著書情報
Article / Book Information

論題(和文)	屈曲に弾性体を用いた空気圧駆動多自由度鉗子マニピュレータ
Title(English)	Pneumatically Driven Multi-DOF Surgical Forceps Manipulator with a Bending Joint Mechanism Using Elastic Bodies
著者(和文)	滝川 恭平, 宮崎 良兼, 菅野 貴皓, 遠藤 玄, 川嶋 健嗣
Authors(English)	Kyouhei Takikawa, Ryoken Miyazaki, Takahiro Kanno, Gen Endo, Kenji Kawashima
Citation(English)	Journal of robotics and mechatronics, Vol. 28, No. 4, pp. 559-567
発行日 / Pub. date	2016, 8
Note	This file is author (final) version.

屈曲に弾性体を用いた空気圧駆動多自由度鉗子マニピュレータ

Pneumatically driven multi-DOF surgical forceps manipulator with a bending joint mechanism using elastic bodies

○滝川　恭平（医科歯科大）宮崎　良兼（医科歯科大）菅野　貴皓（医科歯科大）
遠藤　玄　（東工大）川嶋　健嗣（医科歯科大）

Kyouhei TAKIKAWA,　Tokyo Medical and Dental University,　kyo.student@gmail.com
Ryoken MIYAZAKI,　Tokyo Medical and Dental University
Takahiro KANNO,　Tokyo Medical and Dental University
Gen ENDO,　Tokyo Institute of Technology
Kenji KAWASHIMA,　Tokyo Medical and Dental University

In this study, a pneumatically-driven forceps manipulator was developed for a master-slave-type surgical robot. The proposed manipulator had two flexible joints, one for the bending joint at the tip and the other for transmitting a bending force from the actuators to the wires of the forceps. The manipulator had two degree-of-freedoms (DOFs) of bending driven by only two pneumatic cylinders and a gripper driven by a cylinder. Given the interoperability in real surgery, a mechanism was proposed such that the clean forceps part could be easily attached to and detached from the filthy drive unit. An experiment of the master-slave-system was conducted with the proposed manipulator to verify the tracking performance of the cylinders' position and the bending angle of the forceps manipulator.

***Key Words*:** Surgical robot , Forceps manipulator , Flexible mechanism, Pneumatic system, Wire drive robot

1. Introduction

Recently, laparoscopic surgeries are performed more often than open surgeries to minimize invasions to normal organs that should not be subjected to any damage and to access target organ. Laparoscopic surgeries can also reduce the physical burden on patients and shorten hospitalization periods. They also have a cosmetic advantage, as surgery scars are less conspicuous. However, the limited view field or low resolution of an endoscopic makes it difficult to accurately determine the condition of the organs to be operated. Additionally, due to the low degrees of freedom of forceps and other surgical instruments, it is not easy for the operator to have a sense of force due to the large distance between the tip of the operating portion of the surgical instruments and the handling portion, and thus operability is unsatisfactory. Therefor, laparoscopic surgeries are more difficult than conventional open surgeries and require the operators to use high-level techniques [1][2].

Robots with forceps tips having multiple degrees of freedom are actively studied to reduce the technical burden on the operator. [3][4][5]. The da Vinci is a commercially available tele-operated surgical robot [6]. However, the da Vinci can only be utilized to perform surgery based on visual information. The da Vinci cannot provide a sense of force, and this may increase the risk of unintentional damage to organs by an operator [7][8]. In this study, in order to solve this problem a forceps manipulator was developed. The manipulator utilized the back-drivability of a pneumatic actuator to estimate contact force without the need for an embedded sensor in the forceps [9][10][11]. The manipulator involved an antagonistic drive with two pneumatic cylinders to drive a single degree of freedom system. Hence, the manipulator needs four pneumatic cylinders to realize two degrees of freedom. A surgical robot consists of forceps that require sterilization and washing prior to each surgery, and a drive unit that cannot be washed and therefor must be detached before and after surgery. In the developed forceps manipulator, the four cylinders and four drive wires were connected independently with each other by using connectors, and therefor the detachment and attachment of the parts consume time [9].

In this study, a mechanism of a surgical robot with forceps and drive units that can be easily detached from each other is proposed. Forceps units proposed by previous studies consisted of an attachment connector fixed at the each drive wire that was connected to each actuator. Conversely, in the forceps unit proposed in this study, an elastic body bendable in two directions is mounted on the rear end of forceps and four drive wires are connected to the elastic body. Thus, there is only one connection pint to the drive unit, and this makes the detachment and attachment of the units easy and the drape structure simple. The drive unit bends the elastic body on the rear end of the forceps unit by a parallel link mechanism, which allows motions with two degree of freedom in the pitch and yaw directions. The parallel link mechanism proposed in this study works with two pneumatic cylinders and required fewer actuators than conventional surgical robots.

The paper is organized as follows. In Section 2, the mechanism of the proposed forceps unit and drive unit is explained. The statics of the proposed mechanism are evaluated in Section 3 and dynamics in Section 4. Section 5 discussed the evaluation tests for a master-slave system and its control performance. The conclusions are presented in Section 6.

2. Pneumatically driven forceps manipulator

2.1 Design guideline

The forceps manipulator proposed in this study consists of a sterilized forceps unit, which is inserted into a patient's body, and a drive unit that drives the joints of the forceps unit.

The forceps unit has a bending mechanism with two degree of freedom for bending, where elastic bodies are placed on both the ends of the metal shaft and are connected to each other with four

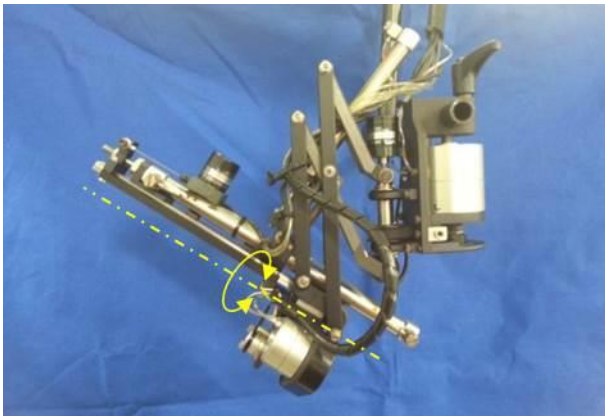

Fig. 1 Robotic forceps holder

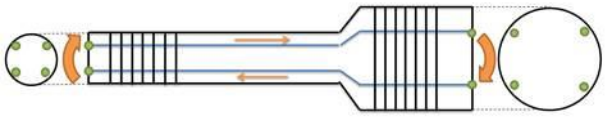

Fig. 2 Manipulator using dual elastic bodies

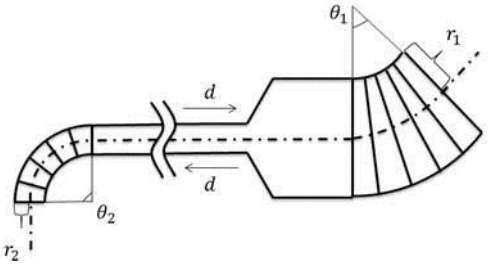

Fig. 3 Displacement magnification mechanism

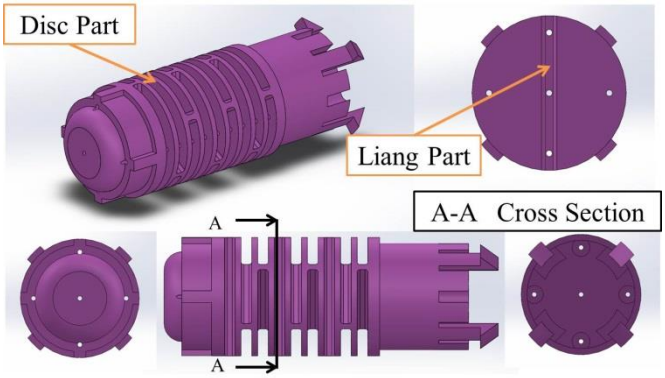

Fig. 4 Rear end of the flexible joint

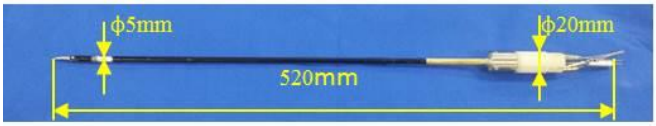

Fig. 5 Forceps unit

wires. When the elastic body on the rear end of the forceps unit is bent, the displacement pulls the drive wire. This in turn bent the elastic body on the front end. The diameter of the tip of the forceps manipulator is 5 [mm], which is approximately the same as that of the widely used forceps. The drive unit has a link mechanism with two degrees of freedom to bend the elastic body on the rear end of the forceps unit. A gimbal joint and a knuckle joint driven with two pneumatic cylinders are proposed, and a prototype is manufactured. The drive unit has a total of three degrees of freedom, namely a degree of freedom for bending. The four degrees of freedom for the translational motion and motion around the roll axis of the forceps are controlled by a conventional holder robot [9] shown in Fig. 1.

The target range of movement of the flexible tip joint is set to ± 60[deg] in the pitch and yaw directions based on the commercial forceps [11].

2.2 Forceps unit with flexible joint

As shown in Fig. 2, with respect to the manipulator's transmission unit, flexible joints of the elastic body structure are fixed on both ends of the rigid body stainless hollow pipe, and the joints are connected with each other by four transmission wires. As depicted in Fig. 3, when the flexible joint on the rear end of the rear end of the manipulator's transmission unit is bent, the wire is pulled and the tension bends the flexible joint on the tip. The flexible joint can bend in the up-down and right-left (yaw and pitch) directions, and two degree of freedom for the bending are realized with the four wires to be connected to four actuators, the proposed forceps only requires a connection between the flexible joint on the rear end and the drive unit for transmission. This reduces the number of parts necessary for attaching and detaching the units and realizes easy attachment and detachment.

It is preferable that the elastic bodies on the tip and the rear end should be rigid against compression and twisting and that they should be flexible for bending. For this purpose, an elastic body of the slit structure consisting of disk parts and beam parts as shown in Fig. 4 is developed. The disks and beams are placed alternately and the angle between adjacent beams is set to 60° to realize bending in two directions. The elastic bodies are made of polypropylene-like material by using a 3D printer of powder sintering type (3D Systems). For the power transmission wires, stand wires (7x7) of SUS304, which are flexible and less resistant against bending are used. The wire diameter is 0.54 [mm]. The front end of the wire is finished with a stainless solder to prevent the wire from slipping out. With respect to the rear end, a brass hollow pipe is pressured and joined with a vice over the wire. As shown in Fig. 3, inter distances (distance between the centers of the parallel wires) of the wires connecting the elastic bodies on the tip and rear end are expressed as r_1 and r_2, respectively, and the corresponding bending angles on the rear end and tip are θ_1 and θ_2 respectively. Therefor the distance and angle satisfy the following equation.

$$\frac{\theta_2}{\theta_1} = \frac{r_1}{r_2} = k_{\mathrm{m}} \qquad (1)$$

Thus, if the value of k_m is chosen appropriately to magnify the displacement, the displacement, the tip can be sufficiently bent even when the movable range of the drive unit and the rear-end flexible joint are small. The target value of the tip bending angle in this study is ± 60 [deg] and the movable range of the drive unit, which will be discussed later, is $-22[\mathrm{deg}] \leq \theta_1 \leq 22[\mathrm{deg}]$. Hence, by assuming that $k_m \geq 3$, the target bending angle can be realized. The prototype of the forceps unit has r_1 =15.6 [mm] on the rear end and r_2 =4.0 [mm] on the tip, and thus, $k_{\mathrm{m}} = 3.9$.

With respect to the gripper at the tip of the forceps, a metal part is mounted on the end of the grasping transmission wire and connected to the grasping drive unit. The gripper is opened and closed by the motion of a compact pneumatic cylinder. The gripper at the tip of the forceps grippes an object by opening and closing two blades with link grooves. The forceps unit prototype has the

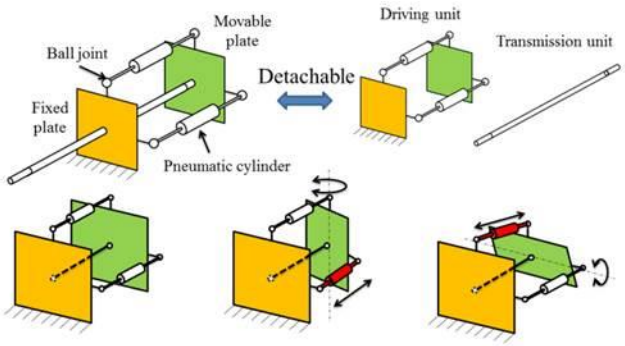

Fig.6 Mechanism of the driving unit

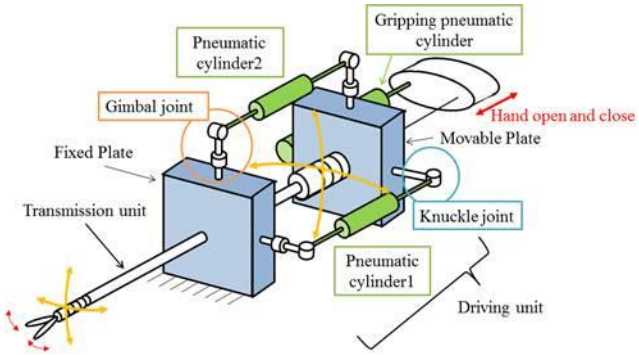

Fig. 7 Overview of the proposed manipulator

following dimensions. The length from the tip of the grasping mechanism of the forceps to the connection mechanism of the drive unit is 520 [mm], the rear end diameter is 20 [mm], and the tip diameter is 5 [mm]. The weight is 50 [g]. The prototype of the forceps unit is shown in Fig. 5.

2.3 Drive unit with two pneumatic cylinders

In the previous study [9], four wires are directly driven with four pneumatic cylinders to realize the above-mentioned two degrees of freedom for the bending motion. Figure 6 shows the drive unit proposed in the present study. The drive unit has a structure involving two plates with a through hole on each plate, with two pneumatic cylinders that connects the two plates to each other. The distance between the plate centers is fixed when the forceps unit is inserted and fixed in the through holes. Hence, the motion of each cylinder generates rotational motions in the yaw or pitch directions. A fixed plate as illustrated in Fig. 6 is mounted on the shaft of the forceps and fixed on the holder robot to prevent a change in its orientation by the cylinder of the drive unit. Conversely, a movable plate is connected to the end of the rear-end flexible joint, and a yaw/pitch motion of the movable plate generated by the cylinder is transmitted to the flexible joint.

However, if the cylinder was simply connected by using a ball joint, then the movable plate could roll unexpectedly about the axis on bending. That is, the fixed plate and the movable plate could twist against each other. The displacement of the cylinder should be used for yaw and pitch motions. Nevertheless, it was partially consumed for the roll motion. This caused a transmission loss that presented accurate motion control.

This type of roll motion problem was also present on the connection part of Souryu I, a connected crawler vehicle for inspecting narrow and winding spaces [13]. In the case of Souryu I, adding a link adding a link mechanism that constrained roll motions

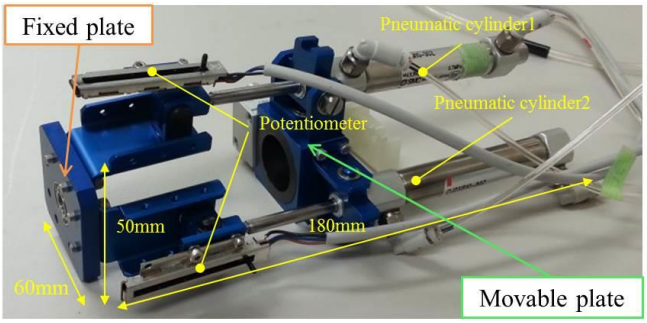

Fig. 8 Proposed driving unit

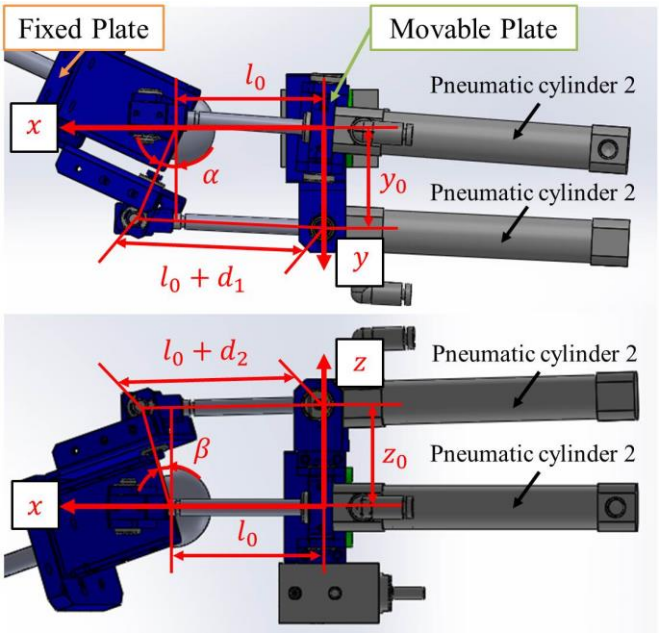

Fig. 9 Relationship between the angle of the position

solved the problem. However, the introduction of such a link mechanism in the forceps manipulator was difficult due to limited space. Therefore, a connection mechanism consisting of three gimbal joints and a knuckle joint as shown in Fig. 7 is used in the present study to prevent roll motions. Pneumatic cylinders (SMC: CJ2XM10-30Z) of inner diameter 10 [mm] and stroke 30 [mm] that allows low-speed drive are used. This specification is necessary since the displacement of the cylinder at the maximum tilting angle ($\pm$22[deg]) of the gimbal joint calculated based on the kinematics is $\pm$ 10 [mm]. Hence, a stroke of 20 [mm] is required. The displacement of the pneumatic cylinders is measured with a linear type potentiometer with stroke limit of 32 [mm] (ALPS: RDC10-320RB), and the pressures of both chambers in the pneumatic cylinders are measured with a pressure sensor (SMC: PSE-510). The dimensions of the drive unit are 180 [mm] x 60[mm] x 50[mm] and the weight is 250 [g]. The prototype of the drive unit is shown in Fig. 8.

This section describes the kinematics of the developed prototype of the forceps manipulator. As in Fig. 9, it is assumed that l_0 is the rod length of the pneumatic cylinders with the movable plate that is not tilted, d_1 and d_2 are the displacements of the pneumatic cylinders 1 and 2, respectively, with the movable plate tilted, and y_0 and z_0 are the dimensions of the link mechanism. According to plane geometry, the bending angles α and β of the movable plate and the displacements d_1 and d_2 of the pneumatic cylinders have

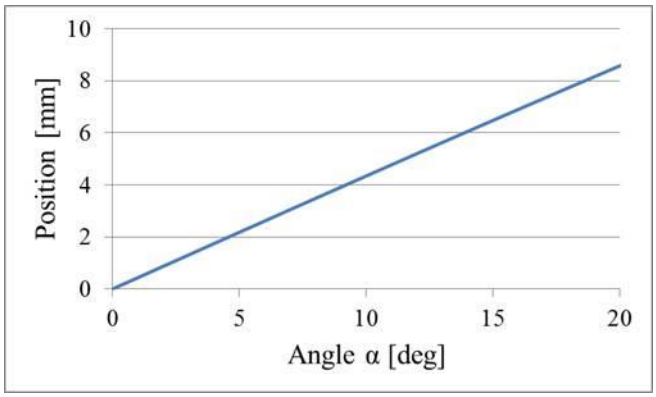

Fig. 10 Relation between the joint angle and cylinder1

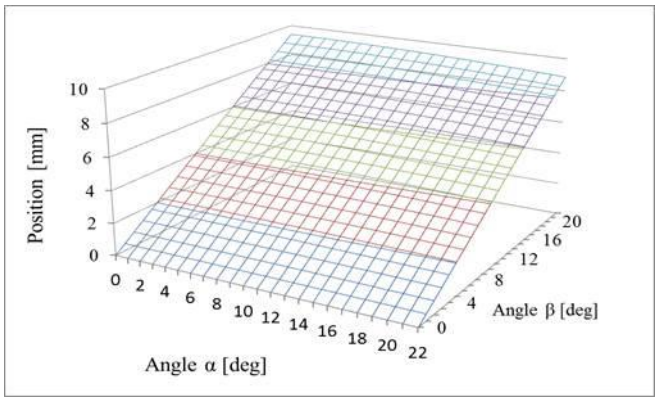

Fig. 11 Relation between the joint angle and cylinder2

the following relation:

$$d_1 = \sqrt{2y_0^2 - 2y_0^2\cos\alpha + l_0^2 + 2l_0\cos\frac{\alpha}{2}\sqrt{2y_0^2 - 2y_0^2\cos\alpha}} + \mathrm{sgn}(\alpha)l_0 \quad (2)$$

$$d_2 = \sqrt{l_0^2 + 2\mathrm{sgn}(\beta)l_0 z_0\cos\alpha\sin\beta + 2z_0^2(1-\cos\beta)} - l_0 \quad (3)$$

Here, sgn(*) is the sign function.

The above equations can be used to obtain the displacement of each pneumatic cylinder from target angles α and β of the movable plate. The tip angle of the forceps unit could be controlled by the position control of the displacement of the cylinders.

The relation between α and the displacement d_1 of the pneumatic cylinder in Eq. (2) is presented in Fig. 10, and the relation between α *or* $\beta$and the displacement d_2 of the pneumatic cylinder in Eq. (3) is presented in Fig. 11. These results indicate a linear relation between the displacement of the pneumatic cylinders and the tip angle. Thus, the controllability would not change primarily based on the displacement. A complete view of the forceps manipulator prototype developed in this study is shown in Fig. 12.

2.4 Configuration of control system

The block diagram of the control system of the pneumatic cylinder of the drive unit is shown in Fig. 13. The system employed a cascade control where a force control loop for the air pressure

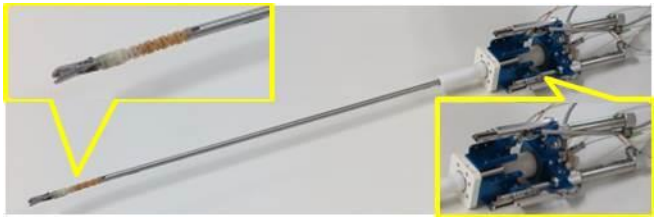

Fig. 12 Transmission unit

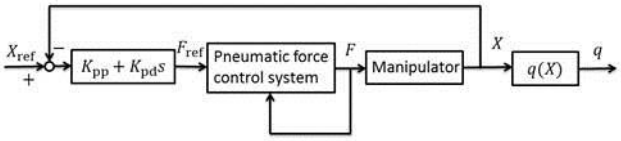

Fig. 13 Block diagram of the joint control system

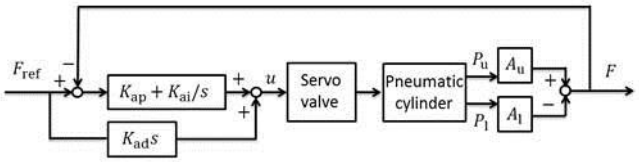

Fig. 14 Block diagram of the pneumatic force control system

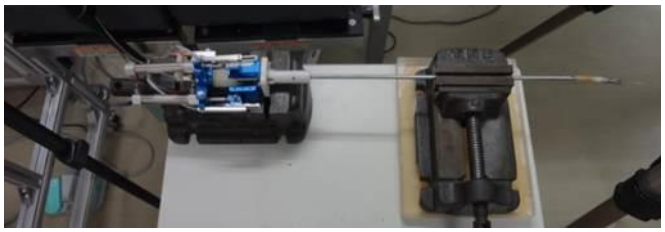

Fig. 15 Experimental setup for evaluation of static characteristics

system was incorporated in the position control loop.

Feed-back of the actual displacement X measured with the potentiometer relative to the target displacement Xref of the cylinder is sent to the PD control of the position. This is then converted by the PD control to the target driving force F_{ref}. In Fig. 13, K_{pp}denotes proportional gain of the position control, K_{pd} denotes differential gain of the position control, and q denotes the bending angle of the joint. The target driving force F_{ref} is generated under the feedback of its error from the actual driving force F. This in turn is calculated from the measurement data of the pressure sensor and by the operation of the servo valve under the PID control as shown in Fig. 14. In the figure, K_{ap} represents the proportional gain of the driving force control, K_{ai}represents the integral gain of the driving force control, u represents the directed voltage of the servo valve, P represents the pressure, and A represents the projected net area of the pneumatic cylinder.

3. Evaluation of statics of the forceps manipulator

3.1 Experiment method

This section evaluated the statics of the forceps manipulator prototype. First, the forceps manipulator was assembled and the target tracking performance of the pneumatic cylinder of the drive unit was verified. Next, the relation between the displacement of the pneumatic cylinder and the bending angle of the drive unit was measured. Finally, the relation between the bending angle of the elastic body on the rear end of the forceps unit and the bending angle of the elastic body on the tip was measured. The transmission

performance obtained from these measurements was compared with the theoretical value of the displacement magnification ratio given by Eq. (1). The displacement of the pneumatic cylinders was measured with a linear potentiometer with a resolution of 0.2 mm.

In the experiments, a stepwise input with an increase of 0.7 [mm] step was provided to the pneumatic cylinders as indicated by the blue solid line in Fig. 16. The input was decreased with the same step as the initial value when the target value reached 10 [mm]. The actual displacement was detected with the potentiometer, as explained in Section 2.2. In the experiment, the fixed plate and the shaft of the forceps manipulator were fixed with a vice as shown in Fig. 15. The target displacement was designated to the pneumatic cylinders 1 and 2, such that the tip of the forceps manipulator bent in the yaw direction and the position control described in Section 2.4 was performed. Given the above target value, the horizontal bending angle $\beta_1$of the movable plate and the horizontal bending angle β_2 of the forceps tip were measured with two fixed cameras. The images taken with the cameras were processed with CAD software (SolidWorks2013) to draw a parallel line to the forceps shaft and a parallel line to the bent forceps tip. The angle between these two lines was then measured. Since the lines were determined visually, the uncertainty of the angle was assumed to be approximately $\pm 1°$. The gains of the control system were set according to Table 1.

Table.1 Gain parameters used in the experiment

$K_{\mathrm{pp}}[\mathrm{N/mm}]$	9.0
$K_{\mathrm{pd}}[\mathrm{N \cdot s/mm}]$	0.1
$K_{\mathrm{ap}}[\mathrm{V/N}]$	0.1
$K_{\mathrm{ai}}[\mathrm{V/(N \cdot s)}]$	0.05
$K_{\mathrm{ad}}[\mathrm{V \cdot s/N}]$	1.2

3.2 Experiment results of statics

Figure 16 shows the target value d_{ref2} [mm] for the displacement of the cylinder 2 and the displacement d_2 [mm] measured with the potentiometer. Figure 17 shows the displacement d_2 [mm] measured with the potentiometer, the angle β_1[deg] between the fixed plate and the movable plate, and a linear approximation equation $\mathrm{y} = 2.32\mathrm{x}$ (with R-squared value of 0.99) of the theoretical curve derived from Eq. (3). The angle β_1 [deg] between the fixed plate and the movable plate and the bending angle β_2 [deg] of the forceps tip are shown in Fig. 18. Figure 19 shows the bending angle β_2 [deg] of the forceps tip and the displacement magnification ratio k_m.

Figure 16 indicated good tracking performance in the position control of the pneumatic cylinders, despite a small stationary error. Figure 17 shows that the displacement of the pneumatic cylinder 2 denoted by X_2 [mm] and the angle of the movable plate β_1 [deg]. The angle followed a straight line as per the linearization formula of the geometrically derived theoretical curve. However, the results illustrated in Figs. 18 and 19 showed that the displacement magnification ratio, which was constant theoretically, was actually dependent on the bending angle in the experiments. This could be because the wire path was shorter when compared with its ideal

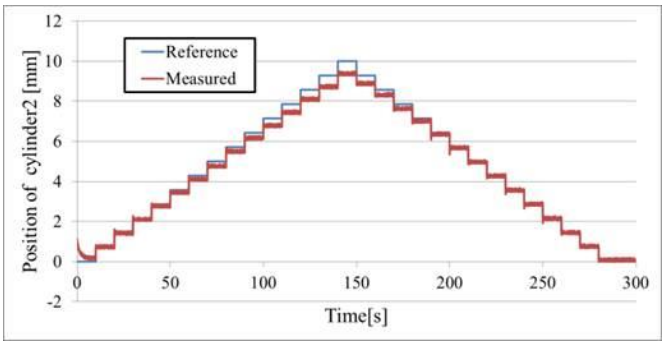

Fig. 16 Results of position control of cylinder2

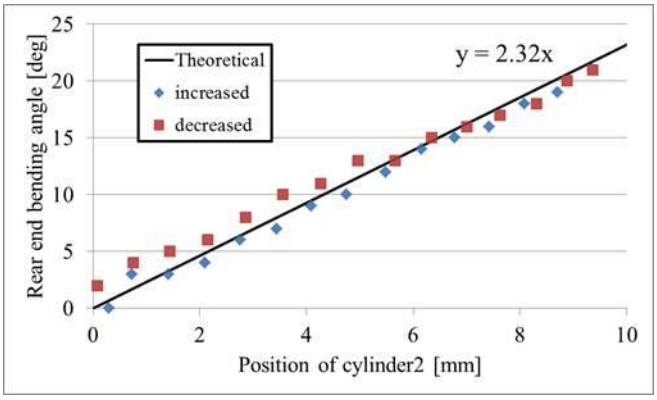

Fig. 17 Results of rear-end bending angle and position of cylinder2

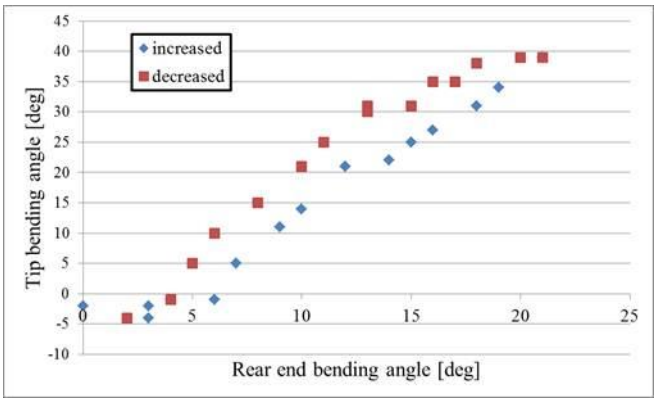

Fig. 18 Results of tip bending angle and rear-end bending angle

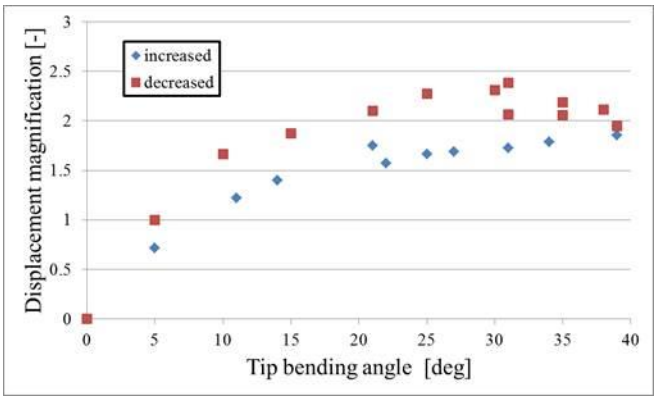

Fig. 19 Results of displacement magnification and bending angle

length due to the presence of a gap between the wire for the bending motion and the wire guide. Additionally, the hysteresis was large because the flexible joints had a hysteresis characteristic. Furthermore, the displacement magnification ratio did not reach 3.9 since the difficulty of applying tension to the wire when assembling

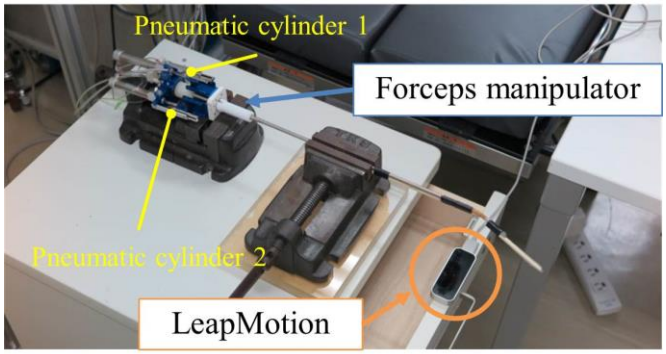

Fig. 20 Experimental setup for evaluation of dynamic characteristics

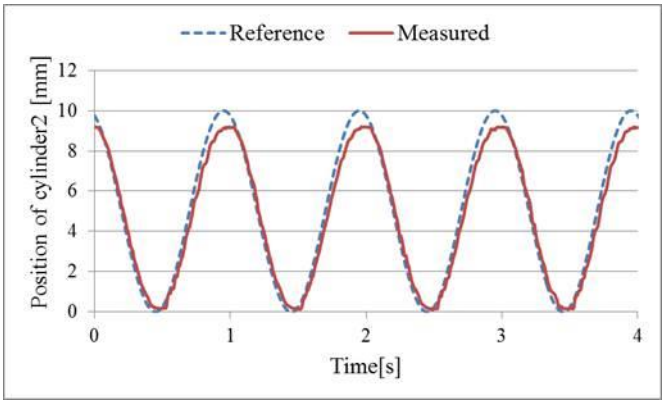

Fig. 21 Results of position control of cylinder2

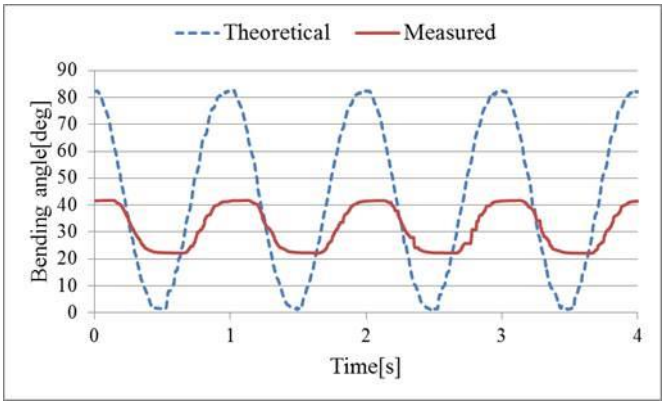

Fig. 22 Results of tip bending angle

the forceps unit caused insufficient wire tension. In addition, the rear-end flexible joint did not move along a uniform arc, as observed in the shot images, and the bending angle per disk was larger on the disks closer to the rear end.

4. Evaluation of dynamics of the manipulator

4.1 Experiment method

Next, the dynamics of the forceps manipulator were experimentally studied to evaluate the effectiveness of the statics (previously discussed in Section 3) in continuous operation. Target values were provided to the forceps pneumatic cylinders 1 and 2 such that the tip moved along a horizontal arc. A motion sensor (LeapMotion: LeapMotion)[14] with a maximum accuracy of 0.01 [mm] was used to measure the movement of the forceps tip and the shaft. The bending angle α_2[deg] of the forceps tip was calculated

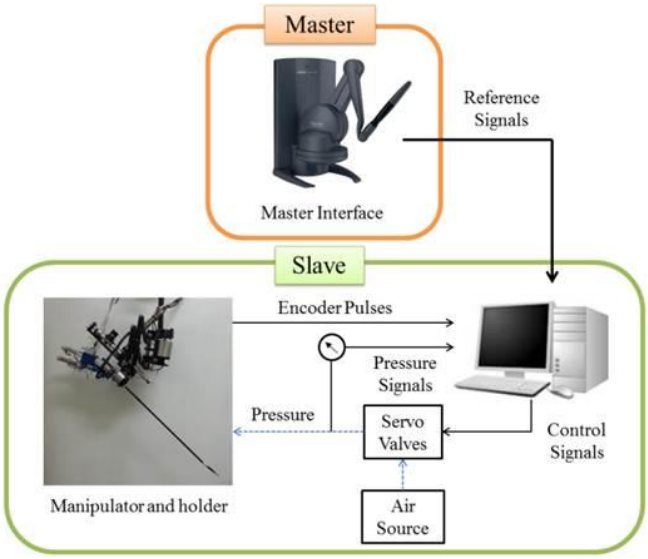

Fig. 23 Overview of the control system

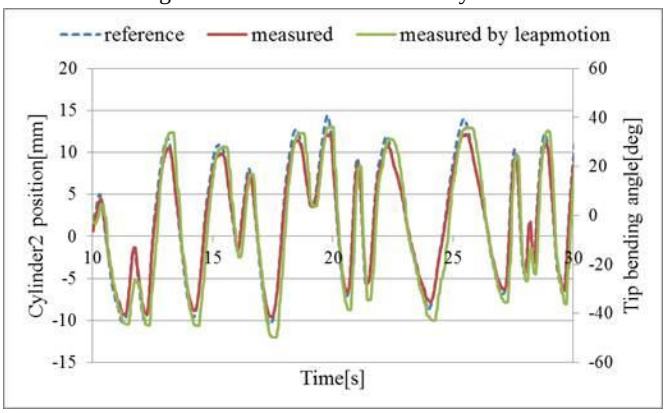

Fig. 24 Results of position control of cylinder2

from the position of the tip, position of the shaft, and position of the rotational center of the flexible joint. The gain parameters used in the experiment were the same as those used in the statics evaluation experiment. Figure 20 shows the evaluation experiment of the dynamics.

4.2 Experimental result of dynamics

Figure 21 shows a target value of the displacement designated for the pneumatic cylinder 2 and the actual data of the displacement of the pneumatic cylinder 2 measured with the potentiometer.

Figure 22 shows the bending angle of the tip of the forceps measured by LeapMotion, and presents its theoretical value. This involved applying Eq. (3) to the displacement of the cylinder to calculate the angle of the movable plate, and then the angle was multiplied with the displacement magnification ratio of 3.9 to calculate the theoretical value of the angle.

The peaks of the sinusoidal wave in Fig. 21 suggested that the target tracking performance reduced as the displacement of the pneumatic cylinder 2 increased. Since the position of the pneumatic cylinders was PD-controlled, the elastic force of the flexible joint increased with the increases in the displacement. Hence, the target value could not be tracked. However, appropriate tracking performance was observed in the areas other than the peaks of the sinusoidal wave.

It could be observed in Fig. 22 that the bending angle of the

forceps tip did not completely return to 0 [deg]. This could be due to the large hysteresis of the tip flexible joint, and as shown in Fig. 21, the displacement in the pneumatic cylinder 2 reached 0 [mm]. The phase delay of the measured data from the theoretical curve could also be attributed to the same cause. The actual measurement values did not reach the peak of the theoretical values probably due to the insufficient tension in the wires when the forceps unit was assembled and the transmission loss caused by the loose wires. These results were the same as those obtained in the statics evaluation experiments.

5. Master slave control experiment

5.1 System configuration

A master-slave system was configured with the developed forceps manipulator prototype as the slave and a commercially available haptic device as the master. The entire system configuration is shown in Fig. 23. When an operator operated the master, a position command value was sent to a control computer of the slave. In the slave, the position control was made according to the command values from the master. The control computer had an AD converter, which read signals from the potentiometer and the pressure sensor and a DA converter that sent control signals to the servo valves.

5.2 Control experiment

A system control experiment was conducted with the master and slave to check the tracking performance of the pneumatic cylinders of the present system. PHANToM Desktop (Sensable) was used as the master unit. Each gain of the control system was set by trial and error as shown in Table 1.

In this experiment, the target tracking performance of the pneumatic cylinder 2 and that of the forceps tip motion were checked with the target values corresponding to the motion created by grasping the operation stick of the master and moving the wrist in the yaw direction. The displacement of the pneumatic cylinders was measured with a linear potentiometer with a resolution of 0.2 [mm] explained in Section 2.3. The bending angle of the forceps tip was measured with the motion sensor LeapMotion detailed in Section 4.1.

Figure 24 shows the target value designated to the pneumatic cylinder 2, actual value measured with the potentiometer, and the bending angle of the forceps tip measured with the LeapMotion sensor. By comparing the target value indicated by a blue dashed line with the measured value indicated by a red solid line, it was confirmed that the actual displacement of the pneumatic cylinders followed the target value of the cylinders in a satisfactory manner. Additionally, the target value was compared with the bending angle of the forceps tip indicated by a green solid line, and it was confirmed that the forceps tip followed the target value of the pneumatic cylinders in a satisfactory manner.

6. Conclusions

In this study, a forceps manipulator mechanism of a master-slave type surgical robot with two pneumatic cylinders was proposed. The forceps unit had a bending mechanism with two degree of freedom for bending, where elastic bodies were placed on both the ends of the metal shaft and were connected to each other with four wires. This allowed two degrees of freedom for the bending motions of the tip of the forceps unit, and realized easy attachment and detachment of the forceps unit and drive unit. The statics and dynamics of the manipulator and the performance of the forceps were evaluated. Furthermore, an experiment involving the master-slave control was conducted. The findings of the experiment indicated that the displacement of the pneumatic cylinders and the bending angle of the tip followed the change in the target value in a satisfactory manner. This could further explored by future research.

Future research includes the development of a forceps unit with a wire tension adjustment mechanism. The mechanism allows sufficiently high tension on the drive wire for the displacement magnification ratio to meet the theoretical value.

Reference

[1] R Berguer, DL Forkey, WD Smith, “Ergonomic problems associated with laparoscopic surgery,” Surgical Endoscopy May 1999, Volume 13, Issue 5, pp 466-468

[2] Gallagher AG, McClure N, McGuigan J, Ritchie K, Sheehy NP, “An Ergonomic Analysis of the Fulerum Effect in the Acquisition of Endoscopic Skills,” Endoscopy. 1998 Sep;30(7):617-20.

[3] Beasley R. A.: Medical Robots: Current Systems and Research Directions, Journal of Robotics, Article ID 401613, 2012.

[4] Russell H. Taylor and Dan Stioianovici, “Medical Robotics in Computer- : Integrated Surgery”, IEEE Trans. on Robotics and Automation, Vol. 19,No. 5, pp. 765-780, 2003

[5] J. Rosen, B. Hannaford, R.M. Satava, “Surgical Robotics Systems Application and Visions,” Springer 2011

[6] Intuitive Surgical Inc, http://www.intuitivesurgical.com/index.aspx

[7] Masaya Kitagawa, Allison M. Okamura, Brian T. Bethea, Vincent L. Gott, William A. Baumgartner, “Analysis of structure manipulation forces for teleoperation with force feedback,” MICCAI 2002 Volume 2488 of the series Lecture Notes in Computer Science pp 155-162

[8] CR Wagner, RD Howe, N Stylopoulos, “The role of force feedback in surgery: analysis of blunt dissection, Haptic Interfaces for Virtual Environment and Teleoperator Systems,” 2002. HAPTICS 2002. Proceedings. 10th Symposium on

[9] K. Tadano, K. Kawashima, “Development of a Master Slave System with Force-Sensing Abilities Using Pneumatic Actuators for Laparoscopic Surgery,” Advanced Robotics, 24(12), pp.1763-1783, 2010

[10] K. Tadano, K. Kawashima, K. Kojima, and N. Tanaka, “Development of a pneumatic surgical manipulator ibis iv. Journal of Robotics and Mechatronics,” Vol. 22, No. 2, pp. 179–188,2010

[11] D. Haraguchi, T. Kanno, K. Tadano, K. Kawashima, “A Pneumatically-Driven Surgical Manipulator with a Flexible Distal Joint Capable of Force Sensing,” IEEE/ASME Transactions on Mechatronics, Vol. 20, No.6, pp.2950-2961, 2015

[12] T. Frede et al., “The Radius Surgical System – A New Device for Complex Minimally Invasive Procedures in Urology,” Lapaproscopy, 51, pp.1015–1022, 2007

[13] T. Takayama, S. Hirose “Development of Souryu I & II -Connected Crawler Vehicle for Inspection of Narrow and Winding Space,” Journal of Robotics and Mechatronics, Vol15, No.1, pp61-69, 2003

[14] Joze Guna, Grega Jakus, Matevz Pogacnik, Saso Tomazic and Jaka Sodnik “An Analysis of the Precision and Reliability of the Leap Motion Sensor and Its Suitability for static and Dynamic Tracking,” Sensors 2014, 14, 3702-3720